Dark Photon Search at BESIII using Initial State Radiation

Maurice Anderson[1,*] on behalf of the BESIII collaboration

[1]Johannes Gutenberg University Mainz, Germany

Abstract. This paper presents a new search at BESIII for the creation and visible decay of a massive dark photon via the initial state radiation process $e^+e^- \to A'\gamma \to l^+l^-\gamma, (l = e, \mu)$. This analysis uses the newly acquired BESIII data on the $\psi(3770)$ resonance with a luminosity of $(20.275 \pm 0.077)\,\mathrm{fb}^{-1}$, currently the world's largest dataset at $\sqrt{s} = 3.773\,\mathrm{GeV}$. The final state l^+l^- invariant mass spectra are scanned to search for a narrow dark photon resonance atop the irreducible QED background. No significant dark photon signal is observed, and new, competitive exclusion limits are set in the mass range below the $\psi(3770)$ resonance.

1 Introduction

One of the greatest unsolved mysteries of modern physics is the observation of invisible yet gravitationally attractive dark matter. The dark photon A', in analogy to the electromagnetic photon, is a proposed new $U(1)$ gauge boson that mediates interactions among dark matter particles and offers a unique vector portal between the Standard Model (SM) and the dark sector. In general, the presence of two $U(1)$ gauge fields in the same Lagrangian leads to a kinetic mixing term, characterized by the dimensionless parameter ε [1]: $\mathcal{L} \supseteq -\frac{\varepsilon}{2} F_{1\mu\nu} F_2^{\mu\nu}$ with the field strength tensors $F_{1\mu\nu} = \partial_\mu A_{1\nu} - \partial_\nu A_{1\mu}$ and $F_2^{\mu\nu} = \partial_\mu A_2^\nu - \partial_\nu A_2^\mu$. Thus, the minimal extension of the SM by introduction of the dark photon leads to a kinetic mixing between the dark photon and the electromagnetic photon. One can diagonalize the kinetic terms of the Lagrangian via rotation and redefinition of the gauge fields [2]. The resulting interaction terms include a coupling between the SM current J_μ and the dark photon A', proportional to ε: $\mathcal{L}_{\mathrm{int}} \supseteq -e\varepsilon J_\mu A'^\mu$. This coupling can be utilized to search for dark photons decaying into visible, SM matter.

At e^+e^- colliders, a massive dark photon could be produced via $e^+e^- \to A'$. This work searches for the subsequent decay into two charged leptons, either via $A' \to e^+e^-$ or $A' \to \mu^+\mu^-$. The irreducible background for such a lepton pair final state is given by the QED processes $e^+e^- \to l^+l^-$, $(l = e, \mu)$ via a virtual, QED photon γ^*. In e^+e^- colliders, the incoming leptons in the initial state always have a nonzero probability to radiate a photon in a process called initial state radiation (ISR). The emitted photon reduces the center-of-mass (CM) energy from $\sqrt{s}$ to $\sqrt{s'} = \sqrt{s(1-x)}$, where $x = \frac{2E_\gamma}{\sqrt{s}}$ is the energy fraction carried off by the ISR photon. This way, a dataset measured at a fixed CM energy can be used to search a large invariant mass range using ISR. This work studies the ISR process $e^+e^- \to A'\gamma \to l^+l^-\gamma$, $(l = e, \mu)$ to search for a dark photon peak atop the irreducible QED background.

*e-mail: maanders@uni-mainz.de

2 BESIII Detector

The BESIII detector [3] records symmetric e^+e^- collisions provided by the BEPCII storage ring [4] in the CM energy range from approximately 2 to 5 GeV, with a peak luminosity of 1.1×10^{33} cm^{-2}s^{-1} achieved at $\sqrt{s} = 3.773$ GeV. Large data samples have been collected in this energy region [5–7]. The cylindrical core of the BESIII detector covers 93% of the full solid angle and consists of a helium-based multilayer drift chamber (MDC), a time-of-flight system (TOF), and a CsI(Tl) electromagnetic calorimeter (EMC), which are all enclosed in a superconducting solenoidal magnet providing a 1.0 T magnetic field. The solenoid is surrounded by an octagonal flux-return yoke made of steel, interleaved with resistive-plate-counter muon-identification modules. The charged-particle momentum resolution at 1 GeV is 0.5%, and the dE/dx resolution is 6% for electrons from Bhabha scattering. The EMC measures photon energies with a resolution of 2.5% (5%) at 1 GeV in the barrel (end cap) region. The time resolution in the plastic scintillator TOF barrel region is 68 ps, while that in the end cap region was 110 ps. The end cap TOF system was upgraded in 2015 using multigap resistive plate chamber technology, providing a time resolution of 60 ps, which benefits about 86% of the data used in this analysis [8–10].

3 Event Selection

In 2017, the BESIII collaboration reported a dark photon search in the mass range 1.5 – 3.4 GeV, in which approximately 2.9 fb^{-1} of data at $\sqrt{s} = 3.773$ GeV was analyzed [11]. No significant dark photon signal was observed, and an upper limit on the kinetic mixing parameter ε was set in the range $10^{-4} - 10^{-3}$ with a confidence level of 90%. This work expands on the previous study by utilizing BESIII's newly accumulated data at $\sqrt{s} = 3.773$ GeV. Following measurements between 2022 and 2024, the total integrated luminosity increased from (2.932 ± 0.014) fb^{-1} [12] to (20.275 ± 0.077) fb^{-1}[13], currently the world's largest dataset at this CM energy. A semi-blind strategy is employed in this work, where only the data samples analyzed in the previous publication (2.9 fb^{-1}) were employed to define the selection conditions. The full dataset (20.3 fb^{-1}) is unblinded only after the selection was frozen and internally validated.

Particle processes are simulated via the Monte Carlo (MC) generators: $e^+e^- \to e^+e^-\gamma$ via Babayaga@NLO [14, 15], $e^+e^- \to \gamma\gamma$ via Babayaga 3.5 [16, 17], $e^+e^- \to \mu^+\mu^-\gamma$ and $e^+e^- \to \pi^+\pi^-\gamma$ via Phokhara 10.0 [18, 19], $e^+e^- \to e^+e^-\mu^+\mu^-$ via DIAG36 [20], and the radiative return (RR) processes $e^+e^- \to \gamma J/\psi$ and $e^+e^- \to \gamma\psi(2S)$ via BesEvtGen [21], which is the BESIII implementation of the EvtGen MC generator [22]. Interactions of particles with the BESIII detector are simulated with GEANT4 [23], and events are reconstructed and analyzed using the BESIII Offline Software System (BOSS) [24].

Events are selected with two well reconstructed tracks in the MDC, corresponding to the charged final state leptons, with a total electric charge of zero. In order to suppress background from $e^+e^- \to \gamma\gamma$ and non-radiative $e^+e^- \to l^+l^-$ events, the opening angle of the tracks must be between 5° and 178°. Electron and muon final states are identified using the ratio of deposited energy E in the EMC and the measured momentum p in the MDC: $0.8 < E/p < 1.2$ for electrons, and $0.05 < E/p < 0.3$ for muons.

ISR photons have the largest probability to be emitted at small polar angles relative to the beam axis and therefore escape undetected. The reconstructed lepton four-momenta are constrained to the $l^+l^-\gamma$ final state hypothesis via a one-constraint (1C) kinematic fit, where the missing photon is required to have zero mass. Only events with the predicted ISR photon emitted at small polar angles (within 0.1 rad of the MDC axis) are accepted.

Fig. 1 shows the invariant mass distributions of the selected e^+e^- and $\mu^+\mu^-$ final states for the semi-blind ($2.9\,\mathrm{fb}^{-1}$) dataset. ISR enables a dark photon search for invariant masses below $\psi(3770)$, while events below about 0.8 GeV cannot be kinematically reconstructed as the boosted leptons escape the detector at small angles undetected. The large data/MC discrepancy at low e^+e^- invariant masses is due to limitations of the Babayaga@NLO generator in simulating next-to-leading (NLO) ISR events involving additional radiation. Pions survive the muon event selection, as these particle types are difficult to kinematically distinguish at BESIII due to their similar masses. The ISR process $e^+e^- \to \pi^+\pi^-\gamma$ is also sensitive to a dark photon kinetic mixing and is therefore included in the subsequent search. The $e^+e^- \to e^+e^-\mu^+\mu^-$ background is smaller than the dominant $\mu^+\mu^-\gamma$ final state by about two orders of magnitude and is therefore deemed as negligible. The J/ψ and $\psi(2S)$ resonances are excluded from the search.

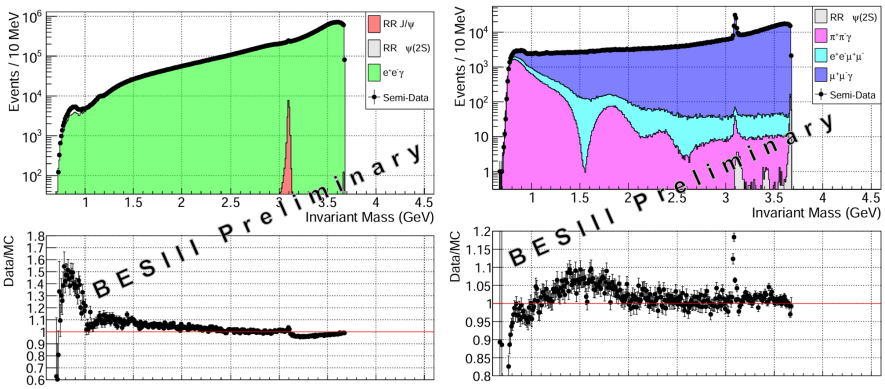

Figure 1. Invariant mass distributions for the final state leptons e^+e^- (left) and $\mu^+\mu^-$ (right). The semi-blind data of the $2.9\,\mathrm{fb}^{-1}$ dataset is plotted with black points. The MC simulations are plotted with stacked histograms, corresponding to the final states: $e^+e^-\gamma$ (green), $\mu^+\mu^-\gamma$ (dark blue), $\pi^+\pi^-\gamma$ (pink), $e^+e^-\mu^+\mu^-$ (cyan), and radiative return to J/ψ (orange) and $\psi(2S)$ (gray). Below are shown the data/MC ratios of the mass distributions.

4 Invariant Mass Spectrum Fits

The resulting e^+e^- and $\mu^+\mu^-$ final state invariant mass spectra are each fitted using a signal-plus-background function in a sliding mass window, where 11 bins with a total width of $\delta m = 110\,\mathrm{MeV}$ are fitted at a time. The background is modeled by a polynomial, while the signal shape is a Crystal Ball function at the center of the mass window, with a width corresponding to the resolution of the l^+l^- invariant mass distribution.

Given an irreducible QED background b_{ll} and a kinetic mixing parameter ε, the amount of expected dark photon signal s_{ll} can be calculated from the ratio of signal ($e^+e^- \to A' \to l^+l^-$) and background ($e^+e^- \to \gamma^* \to l^+l^-$) process integrated cross sections, $\mathrm{d}\sigma_{\mathrm{dark}}$ and $\mathrm{d}\sigma_{\mathrm{QED}}$, respectively [25]. The initial and final state factors cancel in the cross section ratio, leaving the propagator and vertex terms:

$$\frac{s_{ll}}{b_{ll}} = \frac{\mathrm{d}\sigma_{\mathrm{dark}}}{\mathrm{d}\sigma_{\mathrm{QED}}} \Rightarrow s_{ll} = \varepsilon^2 \cdot (b_{ll} \cdot f) \cdot \frac{\pi}{2\tilde{\Gamma}} \cdot \frac{m_{A'}^2}{\delta m}\,, \tag{1}$$

where $\tilde{\Gamma} = \Gamma/\varepsilon^2$ is the ε-independent total decay width, given by the sum of partial decay widths for all possible visible decay channels: $\Gamma = \sum_{l=e,\mu,\tau} \Gamma_{ll} + \Gamma_{\text{hadrons}}$ with $\Gamma_{ll} = \frac{m_{A'}\alpha\varepsilon^2}{3}\sqrt{1-\frac{4m_l^2}{m_{A'}^2}}\left(1+\frac{2m_l^2}{m_{A'}^2}\right)$ and $\Gamma_{\text{hadrons}} = \Gamma_{\mu\mu} \cdot R$. By integrating over the R-ratio $R = \frac{\sigma(e^+e^-\to\text{hadrons})}{\sigma(e^+e^-\to\mu^+\mu^-)}$ [26], the total decay width of A' in the signal-to-background ratio accounts for the leading background contribution $e^+e^- \to \pi^+\pi^-\gamma$, which is sensitive to the hadronic decay $A' \to \pi^+\pi^-$. In radiative Bhabha scattering, a massive dark photon A' can be produced on-shell only in the annihilation process (s-channel), thus the t-channel contribution in the SM background should not be accounted for in the normalization. The factor f, evaluated with the Babayaga@NLO event generator, accounts for the t-channel contribution, providing the corrected scaling of the SM background in the e^+e^- channel.

With b_{ll} corresponding to the integrated background polynomial in the mass window, the Crystal Ball signal shape is constrained such that its integral equals s_{ll}. In every mass window, a fit is performed for different ε values, scanning the range $\varepsilon = 0 - 10^{-2}$. The χ^2 of the fit is defined as $\chi^2 = \sum_{j=i=5}^{i+5} \frac{(n_j-\mu_j)^2}{\sigma^2_{\text{stat},j}+\sigma^2_{\text{sys},j}}$, where the index j runs across the mass bins of the fit window, centered around bin i, n_j is the measured event count, μ_j is the sum of the Crystal Ball and polynomial fit functions, $\sigma^2_{\text{stat},j}$ is the statistical uncertainty of the Poisson-distributed event counts, and $\sigma^2_{\text{sys},j}$ is the systematic variance arising from variation in the analysis choices: bin width, fit window size, and degree of the background polynomial. The relative systematic variance $\sigma^2_{\text{sys},j}/n_j$ for each bin is in the order of 10%. The χ^2 of every fit can be used to define a likelihood $L = e^{-\frac{1}{2}\chi^2}$. Plotting L as a function of the different scanned ε values, the significance of a dark photon signal is given by $Z = \sqrt{-2\ln(L_0/L_{\max})}$, where L_0 is the likelihood value for $\varepsilon = 0$, and $L_{\max}$ is the maximum likelihood. For a background-like mass window, L becomes maximal at $\varepsilon = 0$, whereas in a signal-like window, L is maximal at a nonzero ε value. No significant dark photon is found in the semi-blind (2.9 fb^{-1}) data.

5 Exclusion Limits

An exclusion limit on the kinetic mixing parameter ε is determined. In each mass window, the upper limit $\varepsilon^{\text{limit}}$ of 90% confidence level is determined from the cumulative integral of the normalized, combined likelihood $L^{\text{norm}} = (L_{ee} \times L_{\mu\mu})^{\text{norm}}$ as a function of ε: $\int_0^{\varepsilon^{\text{limit}}} L^{\text{norm}}\,\mathrm{d}\varepsilon = 0.9$. The full dataset of about 20.3 fb^{-1} is analyzed in the same procedure as explained above. No significant dark photon signal is observed with $Z > 3\sigma$ local significance. The resulting exclusion limits on ε for the studied mass range are shown together with the limits of other experiments in Fig. 2.

6 Summary and Conclusions

In summary, after searching for a narrow dark photon signal in the invariant mass spectra of electron and muon pairs produced via initial state radiation, this work reports improved exclusion limits on the kinetic mixing parameter ε, benefiting from the enlarged BESIII dataset of 20.3 fb^{-1} at $\sqrt{s} = 3.773$ GeV. The new limits of this work improve upon the previous results of BABAR [27], BESIII [11], and LHCb [29] for dark photon masses between the $\phi(1020)$ and $\psi(2S)$ resonances. While the limits of KLOE [28] and CMS [30] remain the most exclusive limits in the ranges 0.8 – 1.0 GeV and approximately 1.2 – 2.5 GeV, respectively, this work's new limits complement the other experiments, providing the world's most stringent limits in the mass range 2.54 – 3.61 GeV to date.

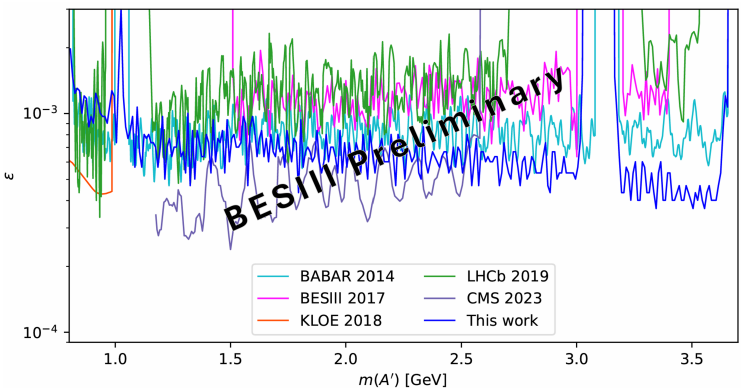

Figure 2. This work's new BESIII exclusion limits on ε, compared to previous limits from BABAR [27], BESIII [11], KLOE [28], LHCb [29], and CMS [30].

References

[1] B. Holdom, Two U(1)'s and Epsilon Charge Shifts. Phys. Lett. B **166**, 196-198 (1986). https://doi.org/10.1016/0370-2693(86)91377-8

[2] M. Fabbrichesi, E. Gabrielli, G. Lanfranchi, The Dark Photon. SpringerBriefs in Physics (2020). https://doi.org/10.1007/978-3-030-62519-1

[3] M. Ablikim *et al.* [BESIII Collaboration], Design and Construction of the BESIII Detector. Nucl. Instrum. Meth. A **614**, 345 (2010). https://doi.org/10.1016/j.nima.2009.12.050

[4] C. H. Yu *et al.*, BEPCII Performance and Beam Dynamics Studies on Luminosity. Proceedings of IPAC2016, Busan, Korea, (2016). https://doi.org/10.18429/JACoW-IPAC2016-TUYA01

[5] M. Ablikim *et al.* [BESIII Collaboration], Future Physics Programme of BESIII. Chin. Phys. C **44**, 040001 (2020). https://doi.org/10.1088/1674-1137/44/4/040001

[6] J. Lu, Y. Xiao, X. Ji, Online monitoring of the center-of-mass energy from real data at BESIII. Radiat. Detect. Technol. Methods **4**, 337–344 (2020). https://doi.org/10.1007/s41605-020-00188-8

[7] J. W. Zhang, L. H. Wu, S. S. Sun *et al.*, Suppression of top-up injection backgrounds with offline event filter in the BESIII experiment. Radiat. Detect. Technol. Methods **6**, 289–293 (2022). https://doi.org/10.1007/s41605-022-00331-7

[8] X. Li *et al.*, Study of MRPC technology for BESIII endcap-TOF upgrade. Radiat. Detect. Technol. Methods **1**, 13 (2017). https://doi.org/10.1007/s41605-017-0014-2

[9] Y. X. Guo *et al.*, The study of time calibration for upgraded end cap TOF of BESIII. Radiat. Detect. Technol. Methods **1**, 15 (2017). https://doi.org/10.1007/s41605-017-0012-4

[10] P. Cao *et al.*, Design and construction of the new BESIII endcap Time-of-Flight system with MRPC Technology. Nucl. Instrum. Meth. A **953**, 163053 (2020). https://doi.org/10.1016/j.nima.2019.163053

[11] M. Ablikim *et al.* [BESIII Collaboration], Dark Photon Search in the Mass Range Between 1.5 and 3.4 GeV/c^2. Phys. Lett. B **774**, 252-257 (2017). https://doi.org/10.1016/j.physletb.2017.09.067

[12] M. Ablikim *et al.* [BESIII Collaboration], Measurement of the integrated luminosities of the data taken by BESIII at $\sqrt{s}$ =3.650 and 3.773 GeV. Chin. Phys. C **37**, 123001 (2013). https://doi.org/10.1088/1674-1137/37/12/123001

[13] M. Ablikim *et al.* [BESIII Collaboration], Measurement of integrated luminosity of data collected at 3.773 GeV by BESIII from 2021 to 2024*. Chin. Phys. C **48** 123001 (2024). https://doi.org/10.1088/1674-1137/ad70a0

[14] G. Balossini *et al.*, Matching perturbative and parton shower corrections to Bhabha process at flavour factories. Nucl. Phys. B **758**, 227-253 (2006). https://doi.org/10.1016/j.nuclphysb.2006.09.022

[15] G. Balossini *et al.*, Photon pair production at flavour factories with per mille accuracy. Phys. Lett. B **663**, 209-213 (2008). https://doi.org/10.1016/j.physletb.2008.04.007

[16] C. M. Carloni Calame *et al.*, Large angle Bhabha scattering and luminosity at flavor factories. Nucl. Phys. B **584** 459-479 (2000). https://doi.org/10.1016/S0550-3213(00)00356-4

[17] C. M. Carloni Calame *et al.*, The BABAYAGA event generator. Nucl. Phys. B Proc. Suppl. **131** 48-55 (2004). https://doi.org/10.1016/j.nuclphysbps.2004.02.008

[18] G. Rodrigo *et al.*, Radiative return at NLO and the measurement of the hadronic cross-section in electron positron annihilation. Eur. Phys. J. C **24** 71-82 (2002). https://doi.org/10.1007/s100520200912

[19] F. Campanario *et al.*, Standard model radiative corrections in the pion form factor measurements do not explain the a_μ anomaly. Phys. Rev. D **100.7** 076004 (2019). https://doi.org/10.1103/PhysRevD.100.076004

[20] F. A. Berends, P. H. Daverveldt, R. Kleiss, Monte Carlo Simulation of Two Photon Processes. 1. Radiative Corrections to Multiperipheral e+ e- mu+ mu- Production. Comput. Phys. Commun. **40** 271-284 (1986). https://doi.org/10.1016/0010-4655(86)90114-1

[21] R. G. Ping, Event generators at BESIII. Chin. Phys. C **32** 599 (2008). https://doi.org/10.1088/1674-1137/32/8/001

[22] D. J. Lange, The EvtGen particle decay simulation package. Nucl. Instrum. Meth. A **462** 152-155 (2001). https://doi.org/10.1016/S0168-9002(01)00089-4

[23] S. Agostinelli *et al.*, GEANT4 - A Simulation Toolkit. Nucl. Instrum. Meth A **506** 250-303 (2003). https://doi.org/10.1016/S0168-9002(03)01368-8

[24] J. Zhang *et al.*, Low transverse momentum track reconstruction based on the Hough transform for the BESIII drift chamber. Radiat. Detect. Technol. Methods **2.1** 20 (2018). https://doi.org/10.1007/s41605-018-0052-4

[25] J. D. Bjorken *et al.*, New Fixed-Target Experiments to Search for Dark Gauge Forces. Phys. Rev. D **80**, 075018 (2009). https://doi.org/10.1103/PhysRevD.80.075018

[26] R. L. Workman *et al.* [Particle Data Group], Review of Particle Physics. PTEP **2022**, 083C01 (2022). https://doi.org/10.1093/ptep/ptac097

[27] J. P. Lees *et al.* [BABAR Collaboration], Search for a Dark Photon in e^+e^- Collisions at BaBar. Phys. Rev. Lett. **113.20**, 201801 (2014). https://doi.org/10.1103/PhysRevLett.113.201801

[28] A. Anastasi *et al.* [KLOE-2 Collaboration], Combined limit on the production of a light gauge boson decaying into $\mu^+\mu^-$ and $\pi^+\pi^-$. Phys. Lett. B **784**, 336-341 (2018). https://doi.org/10.1016/j.physletb.2018.08.012

[29] R. Aaij *et al.* [LHCb Collaboration], Search for $A' \to \mu^+\mu^-$ Decays. Phys. Rev. Lett. **124.4**, 041801 (2020). https://doi.org/10.1103/PhysRevLett.124.041801

[30] A. Hayrapetyan *et al.* [CMS Collaboration], Search for direct production of GeV-scale resonances decaying to a pair of muons in proton-proton collisions at $\sqrt{s} = 13$ TeV. JHEP **12**, 070 (2023). https://doi.org/10.1007/JHEP12(2023)070